

Comparison of Accuracy of Peak Shape Fitting Functions Applied to Airborne Alpha Beta Spectrum

Si Hyeong Sung*, Hee Reyoung Kim

Nuclear Engineering, Ulsan National Institute of Science and Technology

*Corresponding author: shlove912@unist.ac.kr

1. Introduction

If alpha and beta in the air can be measured, real-time monitoring is possible, which can greatly contribute to the radiation safety of nuclear power plant workers. To measure alpha and beta spectra in the air, a detection system was constructed using a PIPS (Passivated Implanted Planar Silicon) detector sensitive to alpha and beta.

However, low-tailing, which occurs due to energy loss after alpha and beta particles interact with a substance, affects the spectrum between nuclides with adjacent peaks, causing spectrum deconvolution, and it is difficult to measure in the air because it causes a decrease in spectral resolution [1].

In this study, when the peak shape fitting equation used for spectrum analysis was applied to the spectrum according to each nuclide, the accuracy was compared and analyzed.

2. Methods

2.1 MCNP-Modeling

The MCNP6 code was used for the simulation, and the PIPS detector was set to 11.95 mm in diameter and 23.9 mm in height based on Canberra's CAM450 model. The filter type was cellulosic asbestos paper, positioned at 20 mm from the detector. The PIPS detector and air filter are inserted inside a box-shaped shield made of stainless steel 304. Nuclides of ^{220}Rn , ^{216}Po , ^{212}Bi and ^{214}Po were set to be uniformly distributed on the cellulose asbestos paper filter. Fig. 1 shows the detection system modeling using MCNP6.

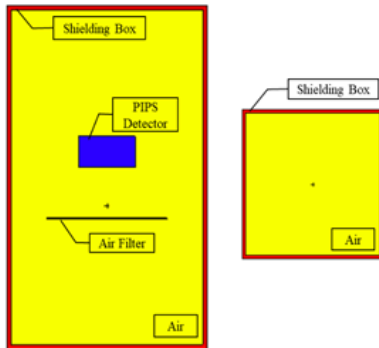


Fig. 1. Detection system MCNP6 modeling

2.2 Equations

The three peak shape fitting functions modified with the exponential equation to fit the low-tailing of alpha

spectrum are shown. Equations (1), (2) and (3) are proposed by L'Hoir (1984), Bortels and Collaers (1987), Koskelo (1996), respectively [2, 3].

$$y(x) = G(x) + T(x)$$

$$\text{Where } G(x) = Hg \times e^{-\frac{(x-xg)^2}{2\sigma^2}}$$

$$T(x) = Hs \times e^{\frac{x-xg}{\sigma \times ts}} \times \text{erfc}\left(\frac{x-xg}{\sqrt{2}\sigma} + \frac{1}{\sqrt{2}ts}\right) \quad (1)$$

$$F(x_i) = He^{-\frac{(x_i-cp)^2}{2\sigma^2}} \quad \text{for } x_i > cp - T$$

$$F(x_i) = He^{\frac{T(2x_i-2cp+T)}{2\sigma^2}} \quad \text{for } x_i < cp - T \quad (2)$$

$$f(u - \mu; \sigma, \tau) = \frac{A}{2\tau} \exp\left(\frac{u-\mu}{\tau} + \frac{\sigma^2}{2\tau^2}\right)$$

$$\times \text{erfc}\left(\frac{1}{\sqrt{2}}\left(\frac{u-\mu}{\tau} + \frac{\sigma}{\tau}\right)\right) \quad (3)$$

3. Results and Discussion

Fig. 2 shows the results of applying the peak shape fitting equation ^{220}Rn progeny spectrum. The accuracy of fitting was confirmed by comparing the RMSE (Root Mean Square Error) value with the reduced chi-square value as in equation (4), (5), respectively. As shown in table I, applying equation (3) shows 26.9 ~ 29.8 % better RMSE than other fitting features. Reduced chi-square value also showed the smallest value. When applied to the actual spectrum, a larger difference in accuracy is expected depending on the degree of overlapping peaks, and it is expected that the real-time alpha measurement accuracy can be improved through peak correction according to the environment.

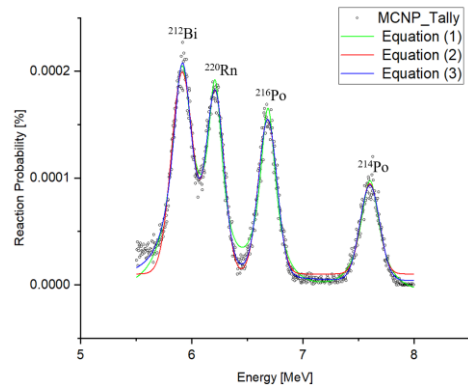


Fig. 2. Fitting functions applied to ^{220}Rn progeny spectrum

$$RMSE = \sqrt{\frac{\sum_{i=1}^n (o_i - c_i)^2}{n}} \quad (4)$$

$$\chi_v^2 = \frac{\chi^2}{\nu} \quad (\chi^2 = \sum_i \frac{(o_i - c_i)^2}{\sigma_i^2}) \quad (5)$$

Table I: Peak shape fitting function accuracy test result

Fitting Function	RMSE	Reduced Chi-Squared Test
Equation (1)	1.02E-05	1.016E-10
Equation (2)	9.97E-06	1.059E-10
Equation (3)	7.86E-06	6.34E-11

Fig. 3 shows the error of each fitting function and the simulation spectrum. The average errors of all energy region of equation (1) to (3) were 7.93E-06 %, 7.97E-06 %, and 5.85E-06 %. Equation (3), which has the highest accuracy, showed the lowest error in the low tailing region of the spectrum. However, the error value increased in the peak and peak overlap region of each nuclide. The maximum error value of the peak increased by 5.22 times compared to the average error value. It judged that the steep peak curve is major cause of low fitting accuracy, and a method of dividing the channel that forms the peak and applying the fitting function is under considering.

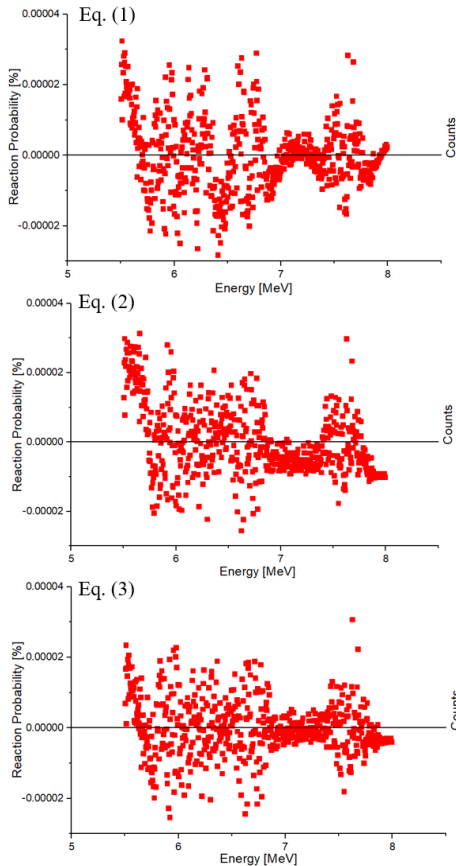


Fig. 3. Error between peak shape fitting function and simulation spectrum

4. Conclusions

In this study, MCNP6 simulation was performed based on the detection system built for the measurement of alpha and beta spectra in air. A peak shape fitting function for reducing the spectral contribution of each nuclide was applied to the simulation results, and accuracy was compared. It is judged that real-time monitoring of alpha and beta in the air will be possible if accurate spectral separation between nuclides is achieved.

NOMENCLATURE

- H : Peak height
- c_p : Centroid
- T : Tailing parameter
- σ : Standard deviation
- Hg : Amplitude of Gauss peak
- xg : Peak channel of Gauss peak
- Hs : Amplitude of peak tailing
- ts : Extent of peak tailing
- x : Channels in interest region
- A : Peak area
- $u - \mu$: Distance to the peak position
- τ : Tailing parameter
- χ_v^2 : Reduced Chi-square
- χ^2 : Chi-square
- σ_i^2 : Variance
- O : MCNP tally value
- C : Calculated value using fitting function
- ν : Degree of freedom

ACKNOWLEDGMENT

This work was supported by the 'Development of Portable Radioactive Contamination Monitoring System for Alpha and Beta Dust Source in the Air' of the Korea Institute of Energy Technology Evaluation and Planning (KETEP) (No. 20171510300590)

REFERENCES

- [1] E.Garcia-Torano, Current status of alpha-particle spectrometry, Appl. Radiat. Isot. 64 (2006) 1273-1280
- [2] Yang, J., L. Zhang, K. Abdumomin, Qiuju Guo, 'Study on peak shape fitting method in radon progeny measurement', Radiation Protection Dosimetry, pp 1-6 (2015)
- [3] S.Pomme, B. Caro Marroyo, 'Improved Peak Shape Fitting in Alpha Spectra', Applied Radiation and Isotopes, vol 96, pp 148-153 (2015)